

Oblate-prolate deformation effect in capture reactions at sub-barrier energiesV. V. Sargsyan,^{1,2} G. G. Adamian,¹ N. V. Antonenko,¹ W. Scheid,³ C. J. Lin,⁴ and H. Q. Zhang⁴¹*Joint Institute for Nuclear Research, RU-141980 Dubna, Russia*²*International Center for Advanced Studies, Yerevan State University, 0025 Yerevan, Armenia*³*Institut für Theoretische Physik der Justus-Liebig-Universität, D-35392 Giessen, Germany*⁴*China Institute of Atomic Energy, Post Office Box 275, Beijing 102413, China*

(Received 16 December 2011; published 17 January 2012)

The role of prolate and oblate deformations of colliding nuclei in the sub-barrier capture process is studied within the quantum-diffusion approach. A comparison of the calculated and measured capture cross sections in the reactions $^{16}\text{O}, ^{48}\text{Ca} + ^{154}\text{Sm}$ and $^{74}\text{Ge} + ^{74}\text{Ge}$ show that transitions during the capture process occur from the potential minimum with an oblate deformation of the ground state to the minimum with a prolate deformation of the nuclei ^{154}Sm and ^{74}Ge . These transitions crucially influence the sub-barrier capture. The capture cross sections and mean-angular momenta are predicted for the reactions of $^{36}\text{S} + ^{170}\text{Er}, ^{174}\text{Yb}$.

DOI: [10.1103/PhysRevC.85.017603](https://doi.org/10.1103/PhysRevC.85.017603)

PACS number(s): 25.70.Jj, 24.10.-i, 24.60.-k

Many investigations cover the role of nuclear deformation in the fusion and capture reactions [1]. The role of deformation becomes more critical especially at the extreme sub-barrier energies [1]. The sensitivity of the capture cross section to the deformations of colliding nuclei gives one the possibility to use these reactions for a deeper understanding of the nuclear structure. From this point of view, it is interesting to investigate the difference between capture reactions with prolate- and oblate-deformed nuclei. If the potential-energy surface has a minimum with an oblate deformation related to the ground state, then there exists a prolate-deformation minimum with almost the same absolute value $|\beta_2|$ of the quadrupole-deformation parameter for the oblate minimum. The energy at the prolate minimum is slightly higher than the energy at the oblate minimum. In heavy-ion collisions, a transition from the ground-state oblate minimum to the prolate minimum of the target nucleus and/or projectile nucleus can take place.

In the present Brief Report, the quantum-diffusion approach [2–4] is applied to study the role of nuclear oblate and prolate quadrupole deformations in sub-barrier capture processes. With this approach, many heavy-ion capture reactions at energies above and well below the Coulomb barrier have been described successfully [2–4]. Since the details of our theoretical treatment were published already in Refs. [2–4], the model is described shortly.

In the quantum-diffusion approach, the collisions of nuclei are treated in terms of a single collective variable: the relative distance between the colliding nuclei. The nuclear-deformation effects are taken into consideration through the dependence of the nucleus-nucleus potential on the deformations and mutual orientations of the colliding nuclei. Our approach takes the fluctuation and dissipation effects in the collisions of heavy ions that model the coupling with various channels (for example, the coupling of the relative motion with low-lying collective modes, such as dynamical quadrupole and octupole modes of the target and projectile [5]) into account. We have to mention that

many quantum-mechanical and non-Markovian effects, which accompany the passage through the potential barrier, are considered in our formalism [2,6] through friction and diffusion. The calculated results for all reactions are obtained with the same parameters as in Refs. [2,4] and are rather insensitive to the reasonable variation of them. One should stress that the diffusion models, which include quantum-statistical effects, also were proposed in Refs. [7–9].

To calculate the nucleus-nucleus interaction potential $V(R)$, we use the procedure presented in Refs. [2–4]. For the nuclear part of the nucleus-nucleus potential, the double-folding formalism with the Skyrme-type density-dependent effective nucleon-nucleon interaction is used. The parameters of the potential were adjusted to describe the experimental data at energies above the Coulomb barrier that corresponds to spherical nuclei. The absolute values of the quadrupole-deformation parameters β_2 of deformed nuclei were taken from Ref. [10].

In Figs. 1(a) and 2, one can see the comparison of the calculated capture cross sections with the available experimental data [11–13] for the reactions $^{16}\text{O}, ^{48}\text{Ca} + ^{154}\text{Sm}$ and $^{74}\text{Ge} + ^{74}\text{Ge}$. There is an experimental confirmation that the nuclei ^{154}Sm and ^{74}Ge have quadrupole oblate deformations [$\beta_2(^{154}\text{Sm}) = -0.341$ and $\beta_2(^{74}\text{Ge}) = -0.2825$] in their ground states [14]. However, our calculations are in good agreement with the experimental data when these nuclei have prolate deformations $\beta_2(^{154}\text{Sm}) = +0.341$ and $\beta_2(^{74}\text{Ge}) = +0.2825$. This indicates that, during the capture process, a transition occurs from the oblate- to the prolate-deformation state of the target nucleus and/or projectile nucleus. The physical reason for such a possibility is that the values of energies of the states with oblate and prolate deformations are very close to each other and the capture with the target and/or projectile nucleus in the prolate minimum is energetically more favorable than the capture with the target and/or projectile nucleus in the oblate minimum.

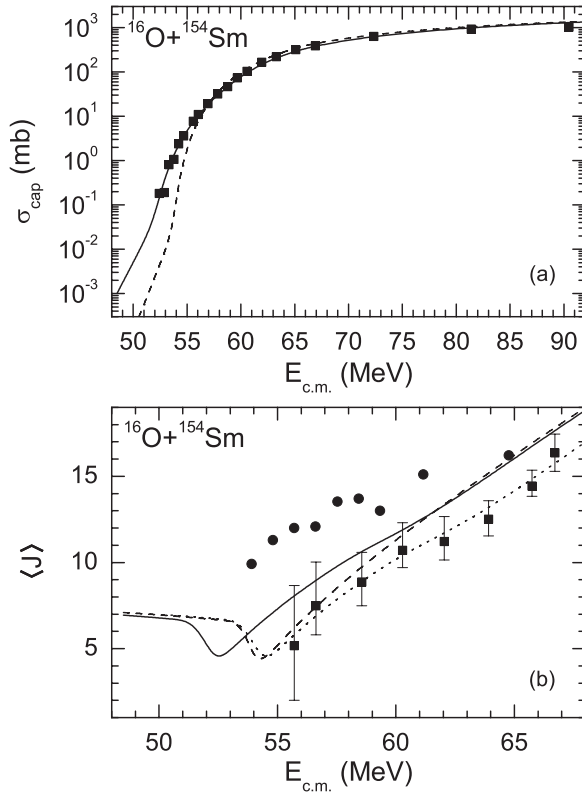


FIG. 1. The calculated (a) capture cross section and (b) mean-angular momentum $\langle J \rangle$ versus $E_{\text{c.m.}}$ for the $^{16}\text{O} + ^{154}\text{Sm}$ reaction are compared with available experimental data [11] (solid squares), [15] (solid circles), and [16] (open squares). The results with a prolate- ($\beta_2 = +0.341$) and oblate- ($\beta_2 = -0.341$) deformed target nucleus ^{154}Sm are shown by solid and dashed lines, respectively. The dotted line in the lower part is calculated with a prolate-deformed target nucleus after shifting the solid curve by 2 MeV in the energy scale. The ^{154}Sm nucleus is oblate deformed in the ground state. The ^{16}O nucleus has $\beta_2 = 0$.

The information about the signs of β_2 for interacting nuclei can also be obtained from the dependence of the mean value of angular momentum $\langle J \rangle$ on the bombarding energy $E_{\text{c.m.}}$. For the $^{16}\text{O} + ^{154}\text{Sm}$ reaction, the comparison between calculated results and two different sets of experimental data [15,16] is shown in Fig. 1(b). As one can see, there is disagreement in the absolute values of the experimental data and theoretical calculations with both a prolate- and an oblate-deformed target nucleus. However, the behavior of the experimental data from Ref. [16] is similar to the theoretical ones when the target nucleus is prolate. Shifting the bombarding energy (or the Coulomb barrier) by 2 MeV, one can get very good agreement between our calculations (dotted line) and the experimental data. This indicates again that the sub-barrier capture takes place with prolate nuclei.

In Fig. 3, the capture cross section, mean-angular momentum $\langle J \rangle$, and the mean square $\langle J^2 \rangle$ versus the bombarding

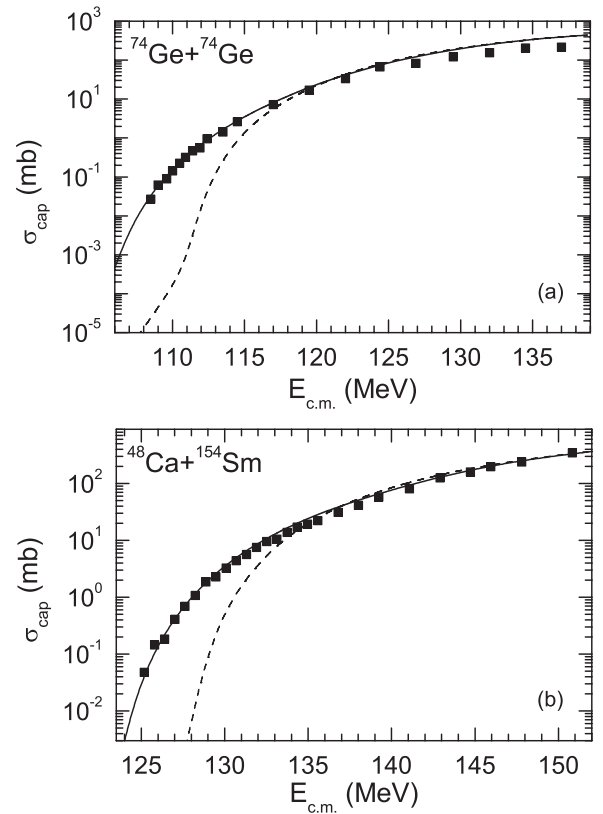


FIG. 2. The calculated capture cross sections versus $E_{\text{c.m.}}$ for the reactions (a) $^{74}\text{Ge} + ^{74}\text{Ge}$ and (b) $^{48}\text{Ca} + ^{154}\text{Sm}$ are compared with available experimental data [13] (solid squares) and [12] (open squares). For the ^{74}Ge nucleus, a prolate $\beta_2 = +0.2825$ (solid line) and oblate $\beta_2 = -0.2825$ (dashed line) deformation is taken. For the ^{154}Sm nucleus, a prolate $\beta_2 = +0.341$ (solid line) and oblate $\beta_2 = -0.341$ (dashed line) deformation is taken. The ^{48}Ca nucleus has $\beta_2 = 0$. The ^{74}Ge nucleus is oblate in the ground state.

energy $E_{\text{c.m.}}$ are predicted for the $^{36}\text{S} + ^{174}\text{Yb}$ reaction. As one can see, the behavior of σ_{cap} , $\langle J \rangle$, and $\langle J^2 \rangle$ is changed, and the minimum of $\langle J \rangle$ or $\langle J^2 \rangle$ is shifted to higher energies when we change the deformation of ^{174}Yb from oblate to prolate.

One can observe the same behavior of σ_{cap} , $\langle J \rangle$, and $\langle J^2 \rangle$ for the $^{36}\text{S} + ^{170}\text{Er}$ reaction (Fig. 4).

For the analyses of capture cross sections for reactions with different Coulomb barrier heights V_b and positions R_b calculated in the case of spherical nuclei, it is useful to compare not the excitation functions, but the dependence of the dimensionless quantities $\frac{\sigma_{\text{cap}} E_{\text{c.m.}}}{\pi R_b^2 \hbar \omega_b}$ and $\frac{\langle J^2 \rangle \pi \hbar^2}{\mu R_b^2 \hbar \omega_b}$ versus $(E_{\text{c.m.}} - V_b)/(\hbar \omega_b)$ or $E_{\text{c.m.}} - V_b$ [3,4,17]. Here, ω_b and μ are the frequency of the barrier approximated by an inverted oscillator and the reduced mass of the system, respectively. Figure 5 shows that the difference between various systems with close deformations is much less than between the same systems but with prolate and oblate deformations of the target nucleus. Since the nuclei ^{170}Er and ^{174}Yb are prolate- and oblate-deformed nuclei in their ground states, respectively,

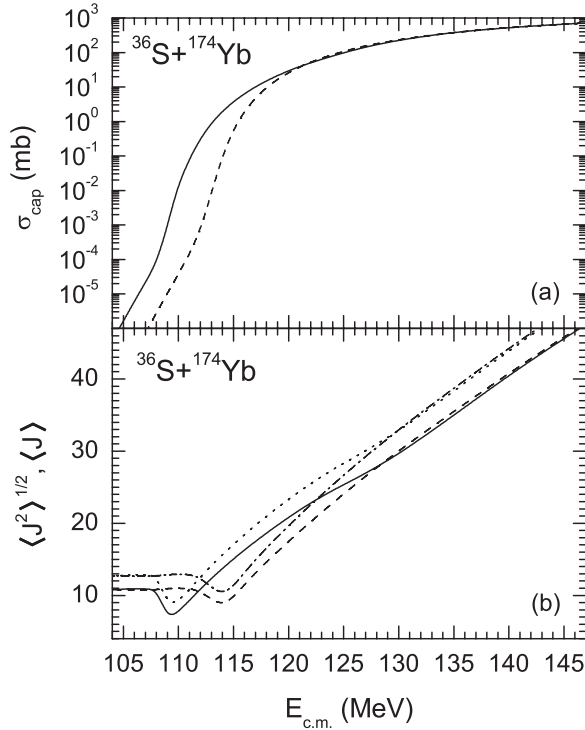


FIG. 3. The calculated (a) capture cross sections and (b) the values of $\langle J \rangle$ and $\langle J^2 \rangle^{1/2}$ versus $E_{c.m.}$ are shown for the $^{36}\text{S} + ^{174}\text{Yb}$ reaction. For the ^{174}Yb nucleus, a prolate $\beta_2 = +0.3249$ (solid line) and oblate $\beta_2 = -0.3249$ (dashed line) deformation is taken. The ^{36}S nucleus has $\beta_2 = 0$. The ^{174}Yb nucleus is oblate in the ground state.

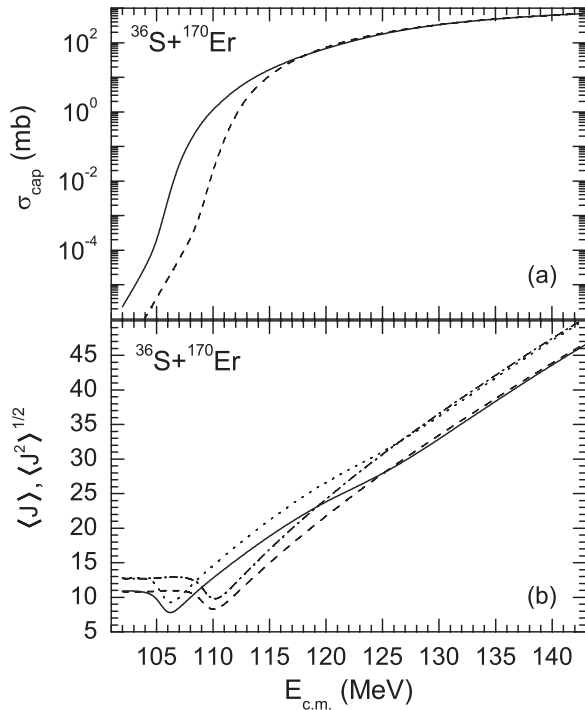


FIG. 4. The same as in Fig. 3 but for the reaction $^{36}\text{S} + ^{170}\text{Er}$. For the ^{170}Er , a prolate $\beta_2 = +0.3363$ (solid line) and oblate $\beta_2 = -0.3363$ (dashed line) deformation is taken. The ^{170}Er nucleus is prolate in the ground state.

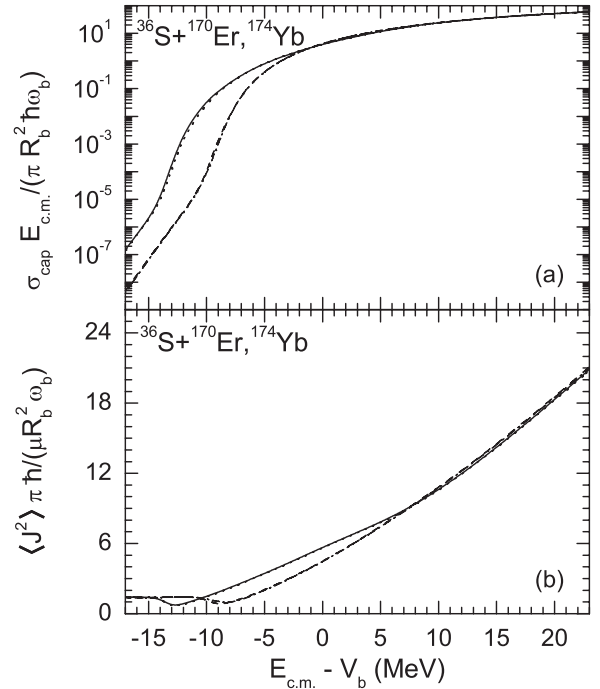


FIG. 5. Comparisons of (a) $\frac{\sigma_{\text{cap}} E_{c.m.}}{\pi R_b^2 \hbar \omega_b}$ and (b) $\frac{\langle J^2 \rangle \pi \hbar^2}{\mu R_b^2 \omega_b}$ versus $E_{c.m.} - V_b$ for the $^{36}\text{S} + ^{170}\text{Er}$, ^{174}Yb reactions. The calculations are presented for the target-nuclei ^{170}Er (prolate), ^{170}Er (oblate), ^{174}Yb (prolate), and ^{174}Yb (oblate) by solid, dashed, dotted, and dashed-dotted lines, respectively.

it may be interesting to compare the reactions $^{36}\text{S} + ^{170}\text{Er}$ and $^{36}\text{S} + ^{174}\text{Yb}$.

The quantum-diffusion approach [2–4] was applied to study the capture process in the reactions with deformed nuclei at sub-barrier energies. From our calculations of the capture process of the reactions ^{16}O , $^{48}\text{Ca} + ^{154}\text{Sm}$ with the oblate-target nucleus, we observed the following information about the deformation properties of nuclei. When the oblate-target nucleus interacts with the reaction partner at sub-barrier energies, the capture takes place rather with the target in the prolate potential minimum than with the oblate-deformed target. Thus, during the capture process, the transition occurs from the oblate-deformation minimum to the prolate-deformation minimum of the target nucleus. The capture with the target nucleus in the prolate potential minimum is energetically more favorable than the capture with the target nucleus in the oblate minimum. This can be approved in the proposed $^{36}\text{S} + ^{170}\text{Er}$, ^{174}Yb experiments.

We thank H. Jia, D. Lacroix and S.-G. Zhou for fruitful discussions and suggestions. This work was supported by the DFG, NSFC, and RFBR. The IN2P3 (France)-JINR (Dubna) and Polish-JINR (Dubna) Cooperation Programmes are gratefully acknowledged.

- [1] A. B. Balantekin and N. Takigawa, *Rev. Mod. Phys.* **70**, 77 (1998); L. F. Canto, P. R. S. Gomes, R. Donangelo, and M. S. Hussein, *Phys. Rep.* **424**, 1 (2006); C. A. Bertulani, *EPJ Web Conf.* **17**, 15001 (2011).
- [2] V. V. Sargsyan, G. G. Adamian, N. V. Antonenko, and W. Scheid, *Eur. Phys. J. A* **45**, 125 (2010).
- [3] V. V. Sargsyan, G. G. Adamian, N. V. Antonenko, W. Scheid, and H. Q. Zhang, *Eur. Phys. J. A* **47**, 38 (2011); *J. Phys.: Conf. Ser.* **282**, 012001 (2011); *EPJ Web Conf.* **17**, 04003 (2011).
- [4] V. V. Sargsyan, G. G. Adamian, N. V. Antonenko, W. Scheid, and H. Q. Zhang, *Phys. Phys. C* **84**, 064614 (2011).
- [5] S. Ayik, B. Yilmaz, and D. Lacroix, *Phys. Rev. C* **81**, 034605 (2010).
- [6] V. V. Sargsyan, Z. Kanokov, G. G. Adamian, N. V. Antonenko, and W. Scheid, *Phys. Rev. C* **80**, 034606 (2009); **80**, 047603 (2009); V. V. Sargsyan, Z. Kanokov, G. G. Adamian, and N. V. Antonenko, *Part. Nucl.* **41**, 175 (2010).
- [7] H. Hofmann, *Phys. Rep.* **284**, 137 (1997); C. Rummel and H. Hofmann, *Nucl. Phys. A* **727**, 24 (2003).
- [8] N. Takigawa, S. Ayik, K. Washiyama, and S. Kimura, *Phys. Rev. C* **69**, 054605 (2004); S. Ayik, B. Yilmaz, A. Gokalp, O. Yilmaz, and N. Takigawa, *ibid.* **71**, 054611 (2005).
- [9] G. Hupin and D. Lacroix, *Phys. Rev. C* **81**, 014609 (2010).
- [10] S. Raman, C. W. Nestor Jr., and P. Tikkanen, *At. Data Nucl. Data Tables* **78**, 1 (2001).
- [11] J. R. Leigh *et al.*, *Phys. Rev. C* **52**, 3151 (1995).
- [12] G. N. Knyazheva *et al.*, *Phys. Rev. C* **75**, 064602 (2007).
- [13] M. Beckerman, M. K. Salomaa, J. Wiggins, and R. Rohe, *Phys. Rev. C* **28**, 1963 (1983).
- [14] [<http://www.nndc.bnl.gov/ensdf/>].
- [15] S. Gil, R. Vandenbosch, A. Charlop, A. Garca, D. D. Leach, S. J. Luke, and S. Kailas, *Phys. Rev. C* **43**, 701 (1991).
- [16] R. Vandenbosch, B. B. Back, S. Gil, A. Lazzarini, and A. Ray, *Phys. Rev. C* **28**, 1161 (1983).
- [17] L. F. Canto, P. R. S. Gomes, J. Lubian, L. C. Chamon, and E. Crema, *J. Phys. G* **36**, 015109 (2009); *Nucl. Phys. A* **821**, 51 (2009).